



Displacement and stress distribution of the maxilla under different surgical conditions in three typical models with bone-borne distraction: a three-dimensional finite element analysis

Yang Shi^{1,2} · Chao-ning Zhu³ · Zhijian Xie^{1,2}

Received: 28 May 2019 / Accepted: 17 January 2020 / Published online: 9 October 2020
© Springer Medizin Verlag GmbH, ein Teil von Springer Nature 2020

Abstract

Objective The present study compared the skeletal effects of surgically assisted rapid maxillary expansion (SARME) with different surgeries in three representative finite element (FE) models.

Study design According to the ossification level of midpalatal suture, three FE models, with different elasticity moduli of sutures ($E = 1$ MPa, 500 MPa, and 13,700 MPa) were constructed, to represent three age groups of patients. Within each model, four groups were set up according to different surgeries: group I (control group without surgery), II (paramedian osteotomy), III (pterygomaxillary separation), and IV (paramedian osteotomy and pterygomaxillary separation). An expansion force of 100 N and 1 mm displacement were applied via a bone-borne distraction to simulate the expansion process.

Results By analyzing these models, the maximum displacement of maxilla was observed in group IV, with $E = 1$ MPa model exhibiting the most displacement (28.5×10^{-6} mm), followed by group II (21.4×10^{-6} mm). Group IV showed a unique backward–downward rotation with minimum stress distributions in three models (9 MPa, 131 MPa, and 140 MPa, respectively), and group II exhibited comparable low stress distributions (12 MPa, 151 MPa, and 230 MPa, respectively). Lowest stress was found in $E = 1$ MPa model, compared with the other two models.

Conclusion There is no need to perform surgeries when the midpalatal suture is open, and surgery guidelines are the same for partial and complete fusion sutures. Furthermore, exclusive use of partial paramedian osteotomy is sufficient enough to reduce stress and expand the posterior part of maxilla, and it is less invasive.

Keywords Minimally invasive osteotomy · Surgically assisted rapid maxillary expansion · Finite element analysis · Palatal expansion technique · Orthodontics, corrective

✉ Zhijian Xie
xzj66@zju.edu.cn

¹ Department of Oral and Maxillofacial Surgery, The Affiliated Stomatology Hospital, Zhejiang University School of Medicine, No. 395, Yan'an Rd, 310003 Hangzhou, China

² Key Laboratory of Oral Biomedical Research of Zhejiang Province, Zhejiang University, 310003 Hangzhou, China

³ State Key Laboratory of Fluid Power and Mechatronic Systems, School of Mechanical Engineering, Zhejiang University, 310058 Hangzhou, China

Verschiebung und Spannungsverteilung des Oberkiefers unter verschiedenen chirurgischen Bedingungen in drei typischen Modellen mit knochengetragener Distraction: eine dreidimensionale Finite-Elemente-Analyse

Zusammenfassung

Zielsetzung In der vorgelegten Studie wurden die skelettalen Auswirkungen der chirurgisch unterstützten schnellen Expansion des Oberkiefers („surgically assisted rapid maxillary expansion“, SARME) mit verschiedenen Operationen in 3 repräsentativen FE(Finite-Elemente)-Modellen verglichen.

Studienaufbau Entsprechend dem Ossifikationsgrad der mittpalatinalen Naht wurden 3 FE-Modelle mit unterschiedlichen Elastizitätsmodulen der Nähte ($E = 1$ MPa, 500 MPa und 13.700 MPa) konstruiert, um 3 Altersgruppen von Patienten zu repräsentieren. Innerhalb jedes Modells wurden 4 Gruppen nach verschiedenen Operationen zusammengestellt: Gruppe I (Kontrollgruppe ohne Operation), II (paramediane Osteotomie), III (pterygomaxilläre Trennung) und IV (paramediane Osteotomie und pterygomaxilläre Trennung). Zur Simulation des Expansionsprozesses wurde eine Expansionskraft von 100 N und eine Verschiebung von 1 mm über eine knochengetragene Distraction angewandt.

Ergebnisse Bei der Analyse dieser Modelle wurde die maximale Verschiebung des Oberkiefers in Gruppe IV beobachtet. Das Modell $E = 1$ MPa wies die größte Verschiebung auf ($28,5 \times 10^{-6}$ mm), gefolgt von Gruppe II ($21,4 \times 10^{-6}$ mm). Gruppe IV zeigte eine besondere Rückwärts-abwärts-Rotation mit minimalen Spannungsverteilungen in 3 Modellen (9, 131 bzw. 140 MPa), Gruppe II zeigte vergleichbar niedrige Spannungsverteilungen (12, 151 bzw. 230 MPa). Die geringste Spannung wurde im Modell $E = 1$ MPa im Vergleich zu den beiden anderen Modellen gefunden.

Schlussfolgerung Es besteht keine Notwendigkeit, Operationen durchzuführen, wenn die mittpalatinal Naht offen ist, und die Operationsrichtlinien sind für partielle und vollständige Fusionsnähte gleich. Darüber hinaus ist die ausschließliche Verwendung einer partiellen paramedianen Osteotomie ausreichend, um die Belastung zu reduzieren und den hinteren Teil des Oberkiefers zu erweitern, und das Verfahren ist weniger invasiv.

Schlüsselwörter Minimal-invasive Osteotomie · Chirurgisch assistierte schnelle Oberkieferexpansion · Finite-Elemente-Analyse · Technik der palatinalen Expansion · Korrigierende Kieferorthopädie

Introduction

Rapid maxillary expansion (RME) has been utilized as an effective treatment for opening the midpalatal suture and correcting transverse maxillary discrepancy for many years [1]. Although it is well-established, some limitations remain for patients with fused midpalatal suture because of the increase in resistance and decrease in elasticity with age [2]. As a result, surgically assisted rapid maxillary expansion (SARME) was introduced in 1938 for nongrowing adolescents and adult patients [3]. SARME helps overcome the obstacles without unwanted adverse effects of conventional RME, such as lateral tipping of teeth and fenestration on the buccal alveolar bone [4].

A wide variety of osteotomy techniques have arisen in recent years to reduce resistance from the surrounding bones. Previous studies showed that the midpalatal and pterygomaxillary sutures were the primary impediments to maxillary expansion [5]. However, proponents of pterygomaxillary disjunction (PMD) believe that SARME with PMD provides long-term stability and enhances the nasal airway [6], but others think SARME without PMD also leads to a sufficient release of impediments for maxillary expansion [7]. Habersack et al. [8] regarded high-resolution multislice computerized tomography (CT) as an effective method to

visualize expansion outcomes in the midpalatal suture and the adjacent sutures, including internasal and nasomaxillary sutures. However, there is no consensus on the surgical guideline, and it still remains a tough judgement for surgeons when deciding which osteotomy technique to choose for each patient.

It is also difficult to determine the minimum age for SARME because many researchers reported that the fusion of the midpalatal suture was not directly associated with age, and no incidence of this kind was discovered in people aged 27 years, 32 years, 54 years or older [9]. Furthermore, no study explored an individual set of surgical procedures for different maturity levels of midpalatal suture.

The present investigation established a three-dimensional (3D) finite element (FE) skull model, and defined the midpalatal suture with three typical mechanical properties. The study explored minimally invasive osteotomy protocols for three different fusion degrees of midpalatal suture, in order to individualize surgical procedure for each patient and achieve the most favorable clinical outcomes.

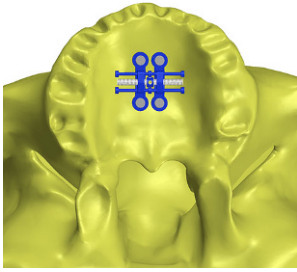


Fig. 1 Visualization of the bone-borne expander position in the palatal view

Abb. 1 Visualisierung der Position des knochengetragenen Expanders in der palatinalen Ansicht

Materials and methods

The geometry of a dry skull with intact craniofacial bones, excluding the mandible and teeth, was digitally reconstructed based on CT images, which were obtained by cone-beam CT. The resulting CT data, in DICOM (Digital Imaging and Communications in Medicine, Arlington, VA, USA) format with a thickness of 0.25 mm per slice, were imported into Mimics 19.0 (Materialise, Leuven, Belgium) for subsequent segmentation. The STL file was then imported into Geomagic Studio 12.0 (3D Systems, Morrisville, NC, USA) to generate a solid 3D geometry. SolidWorks 2016 (SolidWorks Co., Concord, MA, USA) was used to construct the bone-borne appliance (Fig. 1).

The STP file from SolidWorks was imported into ANSYS 15.0 (ANSYS, Inc., Canonsburg, PA, USA) to create and analyze four different models, with each model involving three specific mechanical properties of midpalatal suture. No exact elasticity moduli of midpalatal sutures at different periods of maturity were defined in previous literatures; therefore, we employed three typical elasticity moduli to represent different ossification degrees of suture: (1) unfused ($E = 1 \text{ MPa}$) [10]; (2) partly fused ($E = 500 \text{ MPa}$) [10, 11]; and (3) completely fused ($E = 13,700 \text{ MPa}$) [12], which is equal to the cortical bone. Four computer-aided design (CAD) models, including a control group (group I, with no osteotomy) and three experimental groups (group II: paramedian osteotomy [Fig. 2a]; group III: pterygomaxillary separation [Fig. 2b], and group IV: paramedian osteotomy and pterygomaxillary separation [Fig. 2c]) were established. The corresponding material properties of each component applied in this study were defined according to previous researches [13, 14]. For the stainless-steel part of the expander, modulus of elasticity was chosen as $206,840 \text{ MPa}$, and $E = 113,000 \text{ MPa}$ was used for the titanium parts (mini-implants). For the bony structure, $E = 13,700 \text{ MPa}$ and $E = 3700 \text{ MPa}$ were used for cortical and cancellous bones, respectively. Poisson's ratio for all of

Hier steht eine Anzeige.

the elements was taken as 0.3. The thickness of the sutures involved was set as 0.5 mm.

In particular, we performed the paramedian osteotomy only from the posterior of nasopalatine foramen to the end of midpalatal suture (Fig. 2a) rather than separating the entire midpalatal suture, in order to lower the risk of post-operative complications, such as bleeding and nerve injury.

The maxilla of these 12 models, including the expanders, were meshed automatically into 0.8 mm tetrahedrons, and the rest of the skull was meshed into 2.5 mm tetrahedrons (Fig. 3), with a total of 190,295 nodes and 799,551 elements. All components of the models were considered homogeneous, isotropic, and linearly elastic.

The custom-fabricated bone-borne expander was placed onto the palatal vault of FE models, fixed by 4 mini-implants which were with an 8 mm length and 2 mm diameter. These implants were vertically inserted into the palatal bone (Fig. 1): two between the second premolars and the other two between the first molars, with a distance 3 mm lateral to the midpalatal suture.

The abovementioned simulations were then activated. Kragt et al. [15] stated that when a force was applied to a dry skull, the initial reaction could predict the clinical reaction. Therefore, we chose 1 mm of transverse expansion for simulation. In addition, an expansion force ranging from 70 to 120 N could be measured clinically at the Department of Orthodontics of the University of Ulm [16]. Therefore, we applied a force of 100 N in our study.

The maximum and minimum displacements of the maxilla were measured in the transverse plane (x-axis), sagittal plane (y-axis) and vertical plane (z-axis). In addition, stress distribution within the maxilla was evaluated by measuring von Mises stress (MPa).

Results

Tables 1, 2, and 3 show the displacement of palatal bone expanded by bone-borne expander, and the directions of displacement in the transverse plane (x-axis), sagittal plane (y-axis), and vertical plane (z-axis) are sketched in Fig. 4. Figs. 5, 6, and 7 exhibit von Mises stress distribution, and the maximum values of each group are compared in Fig. 8.

Displacements in the transverse plane

In the transverse plane (x-axis), groups I and II of $E = 1$ MPa model exhibited more displacements in the anterior part of palatal vault, compared with that in the posterior part (Fig. 4a), while groups III and IV showed opposite results, with the posterior part of midpalatal suture opened wider. Among the four groups, the largest displacements produced by the bone-borne expander in the x-axis were found in group II (21.4×10^{-6} mm) and group IV (28.5×10^{-6} mm).

However, when the modulus of elasticity increased to 500 and 13,700 MPa, more segments were achieved in the posterior part of palatal vault in group II (8×10^{-6} mm for

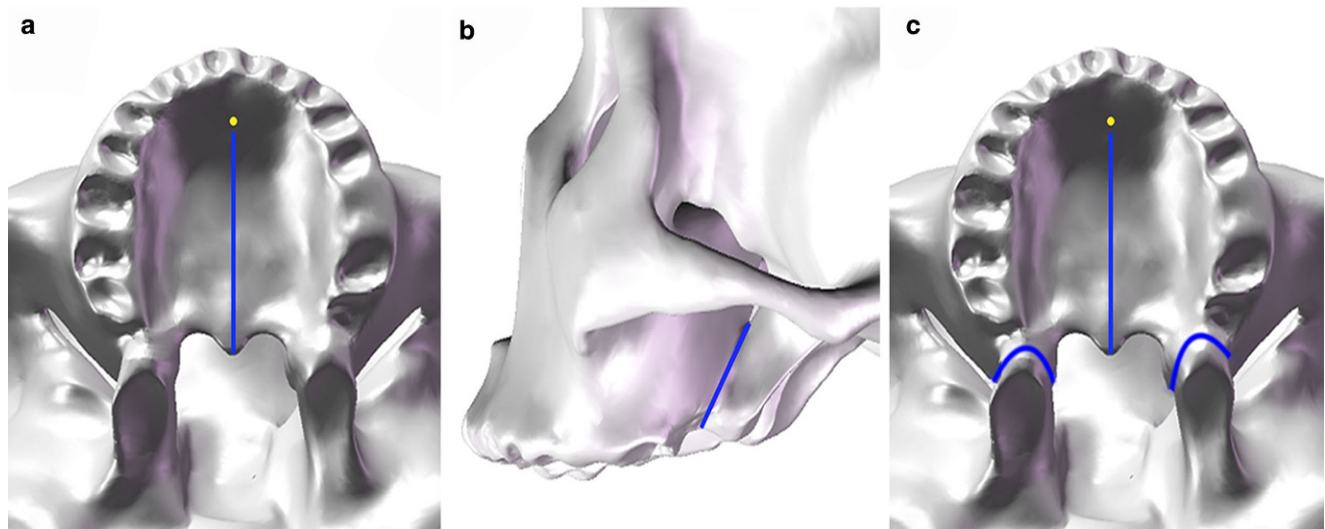


Fig. 2 The CAD (computer-aided design) models with different surgically assisted rapid maxillary expansion (SARME) procedures, the surgical cuts were visualized as blue lines, and the nasopalatine foramen was labeled in yellow dot: **a** group II: paramedian osteotomy (top view); **b** group III: pterygomaxillary separation (lateral view); **c** group IV: paramedian osteotomy and pterygomaxillary separation (top view)

Abb. 2 Die CAD („computer-aided design“)-Modelle mit verschiedenen chirurgisch assistierten schnellen Oberkieferexpansionen (SARME) Verfahren. Die Inzisionen wurden als blaue Linien visualisiert, der Canalis incisivus ist mit einem gelben Punkt markiert: **a** Gruppe II: paramediane Osteotomie (Draufsicht); **b** Gruppe III: pterygomaxilläre Separierung (laterale Ansicht); **c** Gruppe IV: paramediane Osteotomie und pterygomaxilläre Separierung (Aufsicht)

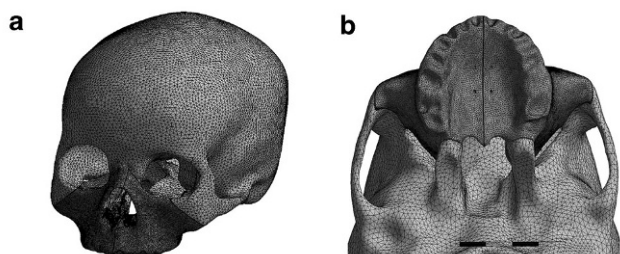


Fig. 3 Meshed finite element model in the study: **a** lateral view, **b** top view

Abb. 3 Das vernetzte Finite-Elemente-Modell in der Studie: **a** Seitenansicht, **b** Draufsicht

500 MPa and 5.6×10^{-6} mm for 13,700 MPa) and group IV (13.2×10^{-6} mm for 500 MPa and 10.2×10^{-6} mm for 13,700 MPa), compared with displacement in the anterior part. In contrast, a larger segment was created in the anterior part of midpalatal suture in group I, which did not undergo surgery. In group III, the largest movement which was caused by the expander occurred around the four implants, with a parallel displacement being observed in the posterior and anterior midpalatal suture (2.1×10^{-6} mm for 500 MPa and 1.3×10^{-6} mm for 13,700 MPa).

Displacements in the sagittal plane

In the sagittal plane (y-axis), results in E=1 MPa model showed that all expansions with surgery procedures induced the maxilla to move forward. This forward movement was greater in group I and group II than that in group III and group IV.

The situation was completely different when the modulus of elasticity was set at 500 and 13,700 MPa, which resulted in a backward movement of the anterior part of palatal bone and a forward shift of the posterior buccal

area. These movements increased from group I to group III, with group III showing the largest displacement of maxilla. However, in group IV, the entire maxilla experienced a backward movement of 9.0×10^{-6} mm for the 500 MPa model and 6.7×10^{-6} mm for the 13,700 MPa model.

Displacements in the vertical plane

In the vertical plane (z-axis), when the midpalatal suture was modelled with a modulus of elasticity of E=1 MPa, the posterior part of the palate in all groups showed a downward displacement with the anterior part moving upwards, which resulted in rotation of the maxilla.

For E=500 MPa and E=13,700 MPa, a similar trend was seen in groups I, II, and III, with the anterior part of the palatal vault moving upwards and the posterior part moving downwards (Fig. 4b). These displacements decreased from group II to group III to group I. Similar to the results for the y-axis, group IV experienced downward movement (2.7×10^{-6} mm for 500 MPa and 2.0×10^{-6} mm for 13,700 MPa).

Patterns of stress distribution

In E=500 MPa model, high stress concentrated around all the placed implants in groups I and III, with a comparable stress value for these two groups (276.46 MPa for group I and 268.9 MPa for group III). A similar phenomenon was also observed for E=13,700 MPa, producing a stress value of 480 MPa for group I and slightly lower stress for group III (410 MPa). Obviously, the von Mises stress in the E=500 MPa model was reduced by half compared to that in the E=13,700 MPa model. While in groups II and IV of these two models, the stress primarily concentrated around the two anterior implants, which meant that the paramedian osteotomy conducted in groups I and II contributed

Table 1 Comparison of maximum (max), minimum (min) as well as mean values of displacements ($\times 10^{-6}$ mm) when elasticity modulus of the midpalatal suture was 1 MPa

Tab. 1 Vergleich der maximalen (max), minimalen (min) und mittleren Werte der Verschiebungen ($\times 10^{-6}$ mm) bei einem Elastizitätsmodul der Sutura palatina mediana von 1 MPa

Group (type of osteotomy)	Transverse plane (x-axis)			Sagittal plane (y-axis)			Vertical plane (z-axis)		
	Min	Max	Mean	Min	Max	Mean	Min	Max	Mean
Group I (no surgery)	-15.8	17.3	16.6	-6.6	-8.5	7.5	-4.1	9.1	6.6
Group II (partial paramedian osteotomy)	-20.3	22.3	21.3	-5.1	-7.5	6.3	-20.8	12.3	16.6
Group III (pterygomaxillary osteotomy)	-18.3	19.4	18.9	-4.5	-4.5	4.5	-15.8	9.6	12.7
Group IV (partial paramedian+ pterygomaxillary osteotomies)	-25.5	31.4	28.5	-1.4	-4.2	2.8	-25.8	10.9	18.4

Transverse plane: The displacement to the right side was regarded as a positive sign while to the left side was indicated as the negative

Sagittal plane: The displacement to the backward direction was regarded as a positive sign and to the forward direction was indicated as the negative

Vertical plane: The displacement to the downward direction was regarded as a positive sign and to the upward direction was indicated as negative

Table 2 Comparison of maximum (max), minimum (min) as well as mean values of displacements ($\times 10^{-6}$ mm) when elasticity modulus of the midpalatal suture was 500 MPa

Tab. 2 Vergleich der maximalen (max), minimalen (min) und mittleren Werte der Verschiebungen ($\times 10^{-6}$ mm) bei einem Elastizitätsmodul der Sutura palatina mediana von 500 MPa

Group (type of osteotomy)	Transverse plane (x-axis)			Sagittal plane (y-axis)			Vertical plane (z-axis)		
	Min	Max	Mean	Min	Max	Mean	Min	Max	Mean
Group I (no surgery)	-2.1	2.0	2.1	-0.4	0.5	0.4	-0.2	0.5	0.3
Group II (partial paramedian osteotomy)	-8.4	7.6	8.0	-3.1	1.8	2.5	-1.9	3.0	2.4
Group III (pterygomaxillary osteotomy)	-2.2	1.9	2.1	-0.6	0.4	0.5	-0.2	0.4	0.3
Group IV (partial paramedian + pterygomaxillary osteotomies)	-14.6	11.6	13.1	7.6	10.3	8.9	-5.1	-0.1	2.6

Transverse plane: The displacement to the right side was regarded as a positive sign while to the left side was indicated as the negative

Sagittal plane: The displacement to the backward direction was regarded as a positive sign and to the forward direction was indicated as the negative

Vertical plane: The displacement to the downward direction was regarded as a positive sign and to the upward direction was indicated as negative

Table 3 Comparison of maximum (max), minimum (min) as well as mean values of displacements ($\times 10^{-6}$ mm) when elasticity modulus of the midpalatal suture was 13,700 MPa

Tab. 3 Vergleich der maximalen (max), minimalen (min) und mittleren Werte der Verschiebungen ($\times 10^{-6}$ mm) bei einem Elastizitätsmodul der Sutura palatina mediana von 13.700 MPa

Group (type of osteotomy)	Transverse plane (x-axis)			Sagittal plane (y-axis)			Vertical plane (z-axis)		
	Min	Max	Mean	Min	Max	Mean	Min	Max	Mean
Group I (no surgery)	-1.1	1.2	1.2	-0.2	0.1	0.2	-0.0	0.3	0.2
Group II (partial paramedian osteotomy)	-5.5	5.5	5.5	-0.0	1.5	0.8	-1.5	2.0	1.8
Group III (pterygomaxillary osteotomy)	-1.2	1.4	1.3	-0.2	0.2	0.2	-0.0	0.5	0.3
Group IV (partial paramedian + pterygomaxillary osteotomies)	-11.2	9.0	10.1	6.9	6.5	6.7	-2.6	-1.3	1.9

Transverse plane: The displacement to the right side was regarded as a positive sign while to the left side was indicated as the negative

Sagittal plane: The displacement to the backward direction was regarded as a positive sign and to the forward direction was indicated as the negative

Vertical plane: The displacement to the downward direction was regarded as a positive sign and to the upward direction was indicated as negative

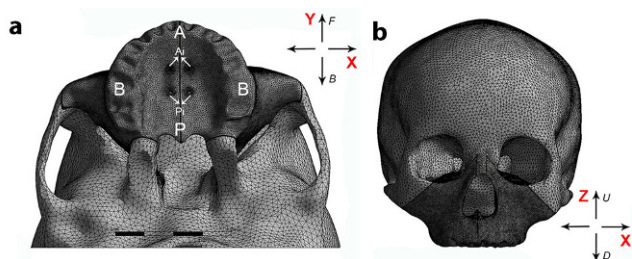


Fig. 4 Schematic drawing of maxilla displacement directions: **a** A anterior part of the maxilla, B buccal part of the maxilla, P posterior part of the maxilla, Ai Anterior implants, Pi Posterior implants, Y y-axis, X x-axis, F forward movement direction, B backward movement direction; **b** Z z-axis, U upward movement direction, D downward movement direction

Abb. 4 Schematische Darstellung der Verschiebungsrichtung des Oberkiefers: **a** A anteriorer Teil des Oberkiefers, B bukkaler Teil des Oberkiefers, P posteriorer Teil des Oberkiefers, Ai anteriore Implantate, Pi posteriore Implantate, Y y-Achse, X x-Achse, F Vorwärtsbewegungsrichtung, B Rückwärtsbewegungsrichtung; **b** Z z-Achse, U Aufwärtsbewegungsrichtung, D Abwärtsbewegungsrichtung

to reduce the stress that concentrated on the two posterior implants (Fig. 4a).

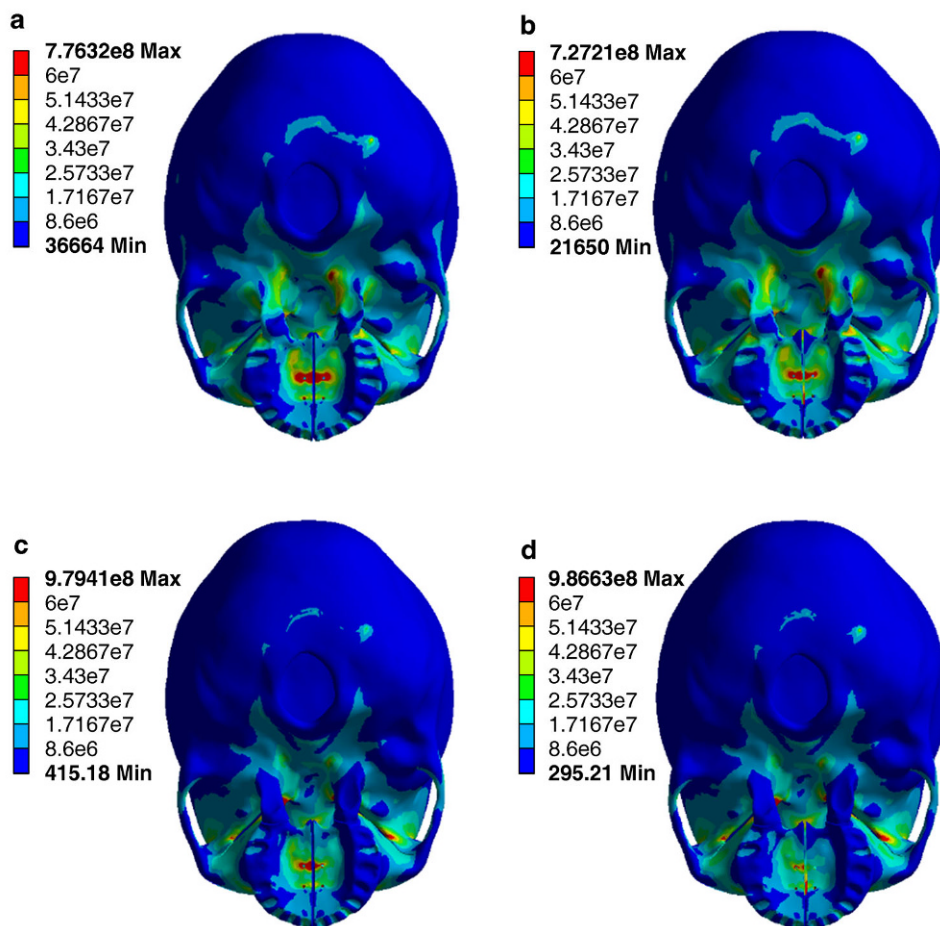
However, compared with $E=500$ MPa and $E=13,700$ MPa models, the stress measured in the $E=1$ MPa model did not exhibit a significant reduction even if osteotomies were employed in group II, group III and group IV, and the maximum stress value of all groups were lower than 30 MPa.

Discussion

Due to the fusion of craniofacial sutures and increased skeletal resistance with age, the predictability of maxillary expansion treatment is greatly reduced. Many types of osteotomies have been reported for rapid maxillary expansion, but there is still no consensus regarding the surgery guidelines for each age groups of patients.

Fig. 5 Distribution of von Mises stress in palatal vault (top view) when $E = 1 \text{ MPa}$: **a** group I (no surgery); **b** group II (paramedian osteotomy); **c** group III (pterygomaxillary separation); **d** group IV (paramedian osteotomy + pterygomaxillary separation)

Abb. 5 Verteilung der Von-Mises-Spannung im Gaumengewölbe (Draufsicht) bei $E = 1 \text{ MPa}$: **a** Gruppe I (keine Operation); **b** Gruppe II (paramediane Osteotomie); **c** Gruppe III (pterygomaxilläre Separierung); **d** Gruppe IV (paramediane Osteotomie + pterygomaxilläre Separierung)



Our investigation demonstrated that for patients with unfused midpalatal suture, the outcomes of maxillary expansion with osteotomies were quite similar to those who did not receive surgery. Likewise, the effectiveness of surgery on reducing stress was quite minor for children compared to that for adolescents and adults. These results indicated that osteotomies should not be excessively performed in children with open sutures. We also found that when no surgery was applied in an unfused model, the midpalatal suture tended to be opened in a parallel manner, and the entire maxilla exhibited a forward-upward rotation, which was consistent with a three-dimensional finite element study conducted by Dalband et al. [17].

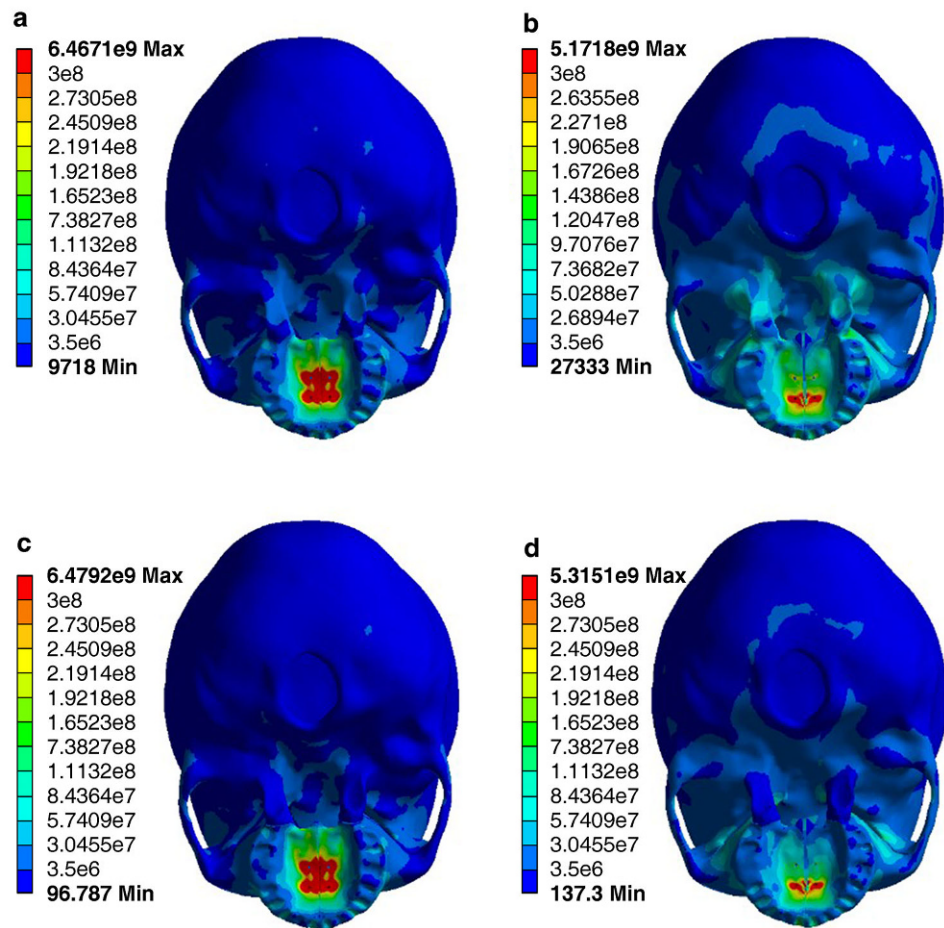
Our results also showed that a majority of displacements occurred in the transverse plane, especially after the paramedian osteotomy combined with pterygomaxillary separation. In adolescent and adult models, we found when no surgery was performed, separation in the anterior part of midpalatal suture was larger than that in the posterior part, which was similar to the results reported by Akkaya et al. [18], primarily because the resistance in the posterior maxilla was greater than that in the anterior. Haas et al. [19]

also found that transseptal fibers connecting the roots of the central incisors were of small elasticity modulus; thus, in clinical treatment, a horizontal V-shaped opening of the midpalatal suture, decreasing from anterior to posterior part, is quite common.

However, osteotomies in our study decreased the resistance from the posterior maxilla, so greater expansion was observed in the posterior part of midpalatal suture, especially in group IV, which was consistent with the study conducted by Lagravere et al. [20], who concluded that more expansion in the posterior part of the suture could be achieved by using more osteotomies. Compared to pterygomaxillary separation, partial paramedian osteotomy facilitated more expansion in the posterior part of the suture, which was consistent with Seeberger et al. [7], who showed that an obvious segment could be established in midpalatal suture even without pterygomaxillary osteotomy. Therefore, to achieve the desirable expansion in the posterior part of the maxilla, a partial paramedian osteotomy is recommended and, if necessary, combined with pterygomaxillary osteotomy. However, if parallel expansion in the midpalatal suture is expected, the exclusive use of pterygomaxillary

Fig. 6 Distribution of von Mises stress in palatal vault (top view) when $E = 500\text{MPa}$: **a** group I (no surgery); **b** group II (paramedian osteotomy); **c** group III (pterygomaxillary separation); **d** group IV (paramedian osteotomy + pterygomaxillary separation)

Abb. 6 Verteilung der Von-Mises-Spannung im Gaumengewölbe (Draufsicht) bei $E = 500\text{MPa}$: **a** Gruppe I (keine Operation); **b** Gruppe II (paramediane Osteotomie); **c** Gruppe III (pterygomaxilläre Trennung); **d** Gruppe IV (paramediane Osteotomie + pterygomaxilläre Trennung)



separation is suggested, which was also reported in previous research [21].

It was clear that midpalatal separation induced greater upward movement of the maxilla in adolescent and adult models, compared with pterygomaxillary osteotomy, which only had little effect on vertical movement. However, when midpalatal separation was combined with pterygomaxillary osteotomy, a complete opposite downward shift occurred, and in the transverse plane, more displacement was found in the posterior palatal vault compared to the anterior area, which was consistent with the FE study performed by Lee et al. [22], who concluded that the maxilla moved primarily downward in a patent-suture model. Therefore, the exclusive use of midpalatal separation is suggested in patients with low vaults, and both surgeries, paramedian osteotomy and pterygomaxillary separation, are required for patients with high vaults.

Notably, the displacement outcomes were similar in the $E = 500\text{MPa}$ and $E = 13,700\text{MPa}$ models. Therefore, it is reasonable to design the same surgical protocol for patients with partial and fully ossified midpalatal sutures. The combination of midpalatal suture separation and pterygomaxil-

lary junction resulted in a backward–downward rotation of the maxilla, with maximum separation of midpalatal suture being achieved in the transverse direction; therefore, when the alveolar ridge is aimed to move lingually and the palatal vault is expected to be lowered, the combination surgical protocol should be used.

When partial midpalatal separation was performed, significantly less von Mises stress was measured, especially with the combination of pterygomaxillary separation, but the synergistic effect was quite minor. Similarly, the exclusive pterygomaxillary separation had little effect on stress reduction in each model. However, Holberg et al. [23] suggested that to protect the cranial base complex from undesirable side effects, separation of the pterygomaxillary junction was a reasonable and necessary additional measure for surgically assisted palatal suture expansion. Our study did not analyze the stress of midface sutures; therefore, further comprehensive studies should be performed to explore the stress distribution around the circummaxillary sutures.

Earlier studies showed that different ossification degrees of circummaxillary sutures in the craniofacial complex

Fig. 7 Distribution of von Mises stress in palatal vault (top view) when $E=13,700\text{MPa}$: **a** group I (no surgery); **b** group II (paramedian osteotomy); **c** group III (pterygomaxillary separation); **d** group IV (paramedian osteotomy + pterygomaxillary separation)

Abb. 7 Verteilung der Von-Mises-Spannung im Gaumengewölbe (Draufsicht) bei $E=13.700\text{MPa}$: **a** Gruppe I (keine Operation); **b** Gruppe II (paramediane Osteotomie); **c** Gruppe III (pterygomaxilläre Separierung); **d** Gruppe IV (paramediane Osteotomie + pterygomaxilläre Separierung)

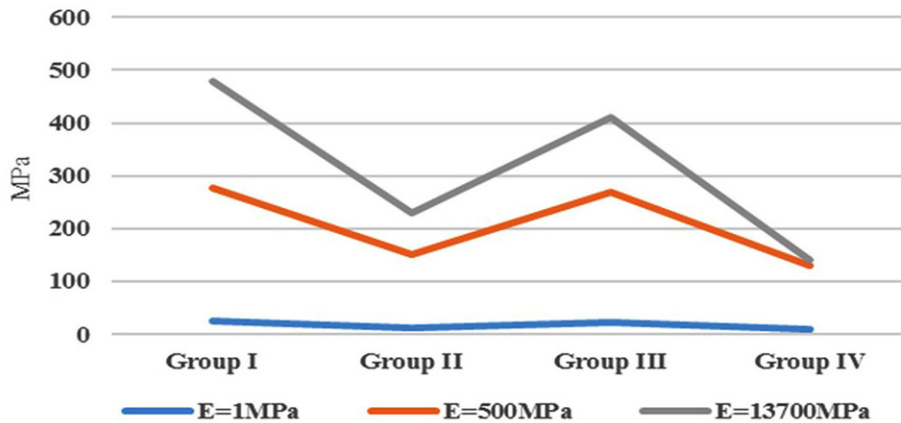
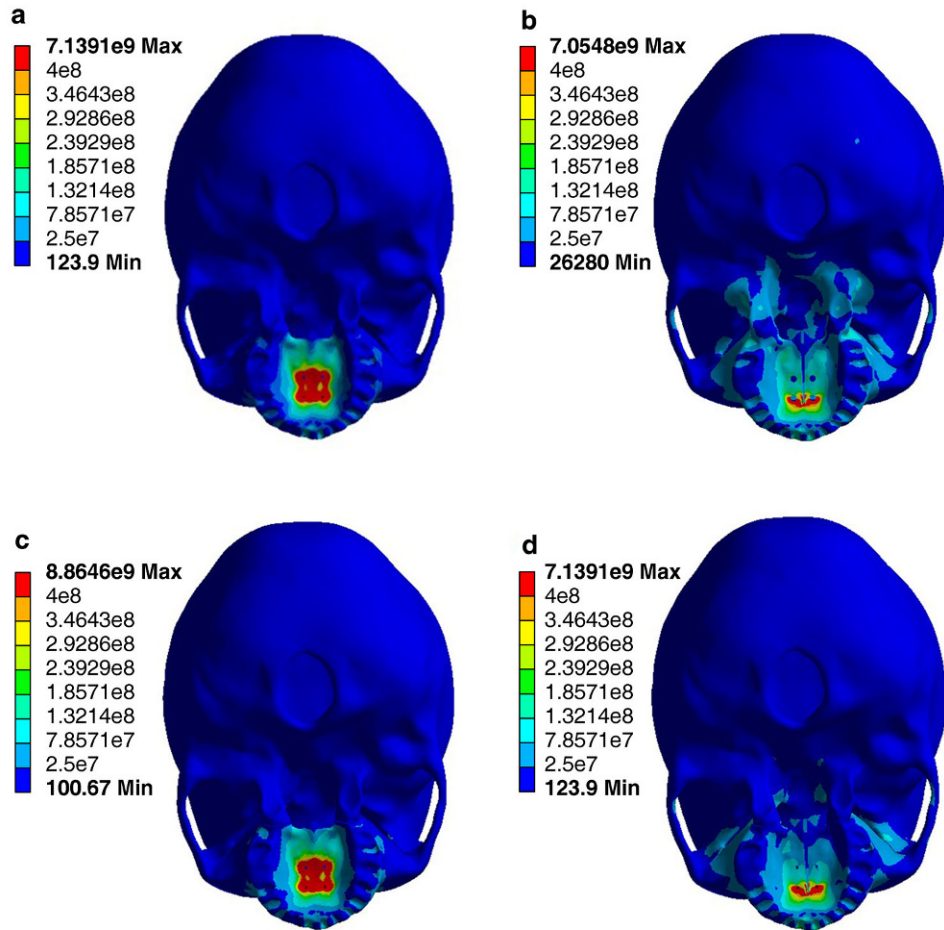


Fig. 8 Line chart of von Mises stress distribution in palatal vault with no surgery (group I), paramedian osteotomy (group II), pterygomaxillary separation (group III), and paramedian osteotomy + pterygomaxillary separation (group IV) in three different elasticity modulus of midpalatal suture models

Abb. 8 Liniendiagramm der Von-Mises-Spannungsverteilung im Gaumengewölbe ohne Operation (Gruppe I), mit paramedianer Osteotomie (Gruppe II), mit pterygomaxillärer Separierung (Gruppe III) und mit paramedianer Osteotomie + pterygomaxillärer Trennung (Gruppe IV) in 3 verschiedenen Elastizitätsmodulen der Modelle der Sutura palatina mediana

resulted in varying outcomes during maxillary expansion [23]. Therefore, we introduced three different elasticity moduli of the midpalatal suture to imitate three typical degrees of ossification, aiming to individualize the surgical procedures for each age group patients. These surgery guidelines will help surgeons to obtain favorable expansion outcomes.

Increasing numbers of surgeons and patients prefer invasive surgical techniques without compromising the clinical outcomes, which has encouraged researchers to explore the perfect surgical protocol. A retrospective cohort study performed by Habersack et al. [24] reported that RME with two osteotomies could achieve a similar clinical result to RME with three osteotomies, and the former greatly reduced the surgical risks and complications. Our investigation also minimized the invasion of midpalatal separation to reduce postoperative complications, such as bleeding, pain and asymmetrical expansion, which may lead to different outcomes compared with other studies.

Nevertheless, one limitation of our study was that the results were obtained from a CAD model, which may decrease the resemblance to clinical situation. Therefore, the FE model can only be used to predict and serve as a reference to help make clinical judgements.

Conclusions

Within the limitations of this FEM investigation, we found no compelling reason to perform any osteotomies when the midpalatal suture is not fused. Once fusion occurs, the surgical guidelines are the same for adolescents and adult patients. In particular, when a greater separation is expected in the posterior area of the midpalatal suture, the exclusive use of partial midpalatal separation is suggested. However, when a backward–downward rotation of the maxilla is required, an additional release of pterygomaxillary junction is recommended, which also presents minimal stress distribution on the maxilla. Therefore, in clinical practice, we suggest that surgeons rationalize the use of SARME based on the midpalatal suture condition and the expected outcomes for individual patients.

Acknowledgements This study has been jointly supported by National Natural Science Foundation of China (Grant Number: 81771118), and Zhejiang Provincial Medical Health Platform Key Project (Grant Number: 2016ZDA015 & 2017KY449). We thank Jue Shi and Mingjie Ge (Department of Oral and Maxillofacial Surgery, The Affiliated Stomatology Hospital, Zhejiang University School of Medicine, Hangzhou 310003, China) for their valuable assistance in improving the English language and quality of figures in this study.

Compliance with ethical guidelines

Conflict of interest Y. Shi, C.-n. Zhu and Z. Xie declare that they have no competing interests.

Ethical standards This study was approved by the Ethics Committee of The Affiliated Stomatology Hospital of Zhejiang University School of Medicine, China, before it was conducted (Number 201921).

References

- Kartalian A, Gohl E, Adamian M, Enciso R (2010) Cone-beam computerized tomography evaluation of the maxillary endosseous complex after rapid palatal expansion. *American journal of orthodontics and dentofacial orthopedics*. *Am J Orthod Dentofacial Orthop* 138:486–492
- Kokich VG (1976) Age changes in the human frontozygomatic suture from 20 to 95 years. *Am J Orthod* 69:411–430
- Brown GVI (1938) The surgery of oral and facial diseases and malformations: their diagnosis and treatment including plastic surgical reconstruction. *JAMA* 112:2199
- Suri L, Taneja P (2008) Surgically assisted rapid palatal expansion: a literature review. *Am J Orthod Dentofacial Orthop* 133:290–302
- Chaconas SJ, Caputo AA (1982) Observation of orthopedic force distribution produced by maxillary orthodontic appliances. *Am J Orthod* 82:492–501
- Koudstaal MJ, Poort LJ, van der Wal KG, Wolvius EB, Prahl-Andersen B, Schulten AJ (2005) Surgically assisted rapid maxillary expansion (SARME): a review of the literature. *Int J Oral Maxillofac Surg* 34:709–714
- Seeberger R, Kater W, Davids R, Thiele OC (2010) Long term effects of surgically assisted rapid maxillary expansion without performing osteotomy of the pterygoid plates. *J Craniomaxillofac Surg* 38:175–178
- Habersack K, Karoglan A, Sommer B, Benner KU (2007) High-resolution multislice computerized tomography with multiplanar and 3-dimensional deformation imaging in rapid palatal expansion. *Am J Orthod Dentofacial Orthop* 131:776–781
- Korbmacher H, Schilling A, Püschel K, Amling M, Kahl-Nieke B (2007) Age-dependent three-dimensional micro-computed tomography analysis of the human mid palatal suture. *J Orofac Orthop* 68:364–376
- Provatis CG, Georgiopoulos B, Kotinas A, McDonald JP (2008) Evaluation of craniofacial effects during rapid maxillary expansion through combined in vivo/in vitro and finite element studies. *Eur J Orthod* 30:437–448
- Gautam P, Valiathan A, Adhikari R (2007) Stress and displacement patterns in the craniofacial skeleton with rapid maxillary expansion: a finite element method study. *Am J Orthod Dentofacial Orthop* 132:5e1–e11
- Tanne K, Hiraga J, Sakuda M (1989) Effects of directions of maxillary forces on biomechanical changes in craniofacial complex. *Eur J Orthod* 11:382–391
- Mahoney E, Holt A, Swain M, Kilpatrick N (2000) The hardness and modulus of elasticity of primary molar teeth: an ultra-micro-indentation study. *J Dent* 28:589–594
- Verrue V, Dermaut L, Verheghe B (2001) Three-dimensional finite element modeling of a dog skull for the simulation of initial orthopedic displacements. *Eur J Orthod* 23:517–527
- Kragt G, Duterloo HS, Ten Bosch JJ (1982) The initial reaction of a macerated human skull caused by orthodontic cervical traction determined by laser metrology. *Am J Orthod* 81:49–56

16. Sander C, Huffmeier S, Sander FM, Sander FG (2006) Initial results regarding force exertion during rapid maxillary expansion in children. *J Orofac Orthop* 67:19–26
17. Dalband M, Kashani J, Hashemzahi H (2015) Three-dimensional finite element analysis of stress distribution and displacement of the maxilla following surgically assisted rapid maxillary expansion with tooth- and bone-borne devices. *J Dent* 12:298–306
18. Akkaya S, Lorenzon S, Uçem TT (1998) Comparison of dental arch and arch perimeter changes between bonded rapid and slow maxillary expansion procedures. *Eur J Orthod* 20:255–261
19. Haas AJ (1965) The treatment of maxillary deficiency by opening the midpalatal suture. *Angle Orthod* 35:200–217
20. Lagravère MO, Major PW, Flores-Mir C (2006) Dental and skeletal changes following surgically assisted rapid maxillary expansion. *Int J Oral Maxillofac Surg* 35:481–487
21. Möhlhenrich SC, Modabber A, Kamal M, Fritz U, Prescher A, Hölzle F (2016) Three-dimensional effects of pterygomaxillary disconnection during surgically assisted rapid palatal expansion: a cadaveric study. *Oral Surg Oral Med Oral Pathol Oral Radiol* 121:602–608
22. Lee H, Ting K, Nelson M, Sun N, Sung SJ (2009) Maxillary expansion in customized finite element method models. *Am J Orthod Dentofacial Orthop* 136:367–374
23. Holberg C, Steinhäuser S, Rudzki I (2007) Surgically assisted rapid maxillary expansion: midfacial and cranial stress distribution. *Am J Orthod Dentofacial Orthop* 132:776–782
24. Habersack K, Becker J, Ristow O, Paulus GW (2014) Dental and skeletal effects of two-piece and three-piece surgically assisted rapid maxillary expansion with complete mobilization: A retrospective cohort study. *J Oral Maxillofac Surg* 72:2278–2288